Bull. Disas. Prev. Res. Inst., Kyoto Univ., Vol. 35, Part 4, No. 316, December, 1985

Soil Movements Associated with Tunneling and Their Effects on an Adjacent Pile Foundation

By Atsushi YASHIMA, Toru SHIBATA, Hideo SEKIGUCHI and Mitsuyoshi KOHNO

(Manuscript received September 24, 1985)

Abstract

The aim of this paper is to clarify the effect of tunneling in sand deposits upon the adjacent, existing structures with pile foundations. For this purpose, a series of laboratory model tests with a lowering-panel are performed. The lowering-panel is placed at the base of a container, on which an assembly of aluminum rods is made to rest, with or without a model pile-foundation being installed. The localized settlement to be created due to tunneling is simulated by allowing the lowering-panel to settle at a given rate. The associated displacement fields above the lowering-panel are measured by means of photographic techniques, and their correlation with the measured pile movements are discussed in detail. Furthermore, these experimental results are compared with results predicted from a new type of finite element analysis making full use of joint elements. It is then shown that there is good correlation between the measured and calculated results.

1. Introduction

The land utilization in most urban areas in Japan has been extensive, and is nowadays almost saturated. Therefore, when the construction of a new large-scale structure is planned in such urban areas, the first thing for the geotechnical engineer to do is to assess how the construction work (mostly excavation work) will affect the performance of the adjacent, existing structures.

The related, important fact is that when the subsoil is excavated for the purpose of construction, a "loosened" zone is almost always created in its neighorhood. This means that if there are adjacent structures within the affected region, they are very likely to suffer from significant damages due to the associated differential settlements and/or horizontal movements of the ground.

Thus, considerable efforts have been so far directed toward establishing methods for predicting the soil movements associated with tunneling[1),2),3)].

For example, Shimada[3)] derived a semi-empirical equation for the transversal settlement, $\delta(x)$, of a generic point $(x=x)$ at the ground surface (see **Fig. 1**). This equation can be expressed, in terms of the tunnel settlement (δ_T), the tunnel radius (a), and of the overburden depth (H), as follows.

$$\delta(x)=A\cdot\delta_T \exp\left[-c_1\cdot(x/H)^2-c_2\cdot(H/a)\right] \quad \cdots\cdots(1)$$

Here, A, c_1, and c_2 are constants to be determined on the basis of field measurements.

Although the soil movements associated with tunneling have received increasing attention as stated above, there are very few in the literature who tackle the effect

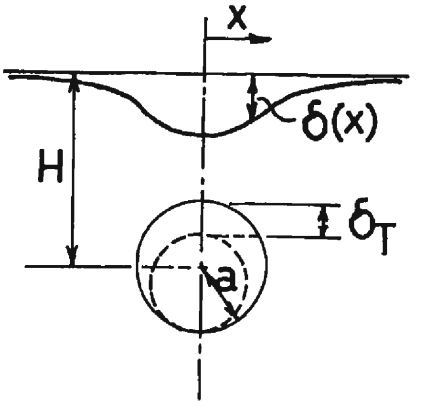

Fig. 1 Transversal settlement at the ground surface

of tunneling on an adjacent pile foundation. This trend seems quite strange, in view of the fact that this problem is of considerable practical significance in urban areas developed on soft alluvial deposits where important structures are commonly supported by pile foundations.

Thus, the present study is aimed at clarifying the effects of soil movements associated with tunneling, upon its adjacent pile foundations. More specifically, the study consists of two related approaches. In the first approach, a series of laboratory lowering-panel tests with a granular medium are performed. The displacement fields above the lowering-panel and their correlation with the pile movement are studied in detail. In the second approach, an appliaction is made of a new type of analysis procedure making full use of joint elements, to reproduce the discrete nature of the granular medium and its consequence upon the displacement field associated with the lowering-panel settlement. In what follows, the results from these approaches will be described in due course.

2. Lowering-Panel Tests with a Granular Medium

2.1 Test Apparatus and Test Procedure

An assembly of aluminum rods with their axes horizontal was used in this experimental program as a two-dimensional model for sandy ground. The advantage of the use of such an assembly of aluminum rods is summarized as follows[4]. Firstly, it makes both front and rear walls of its container unnecessary and the influence of wall friction is thereby removed. Secondly, it permits a detailed observation of the displacement field of the granular medium, at a particle level, when coupled with relevant photographic techniques.

The test apparatus used is shown in **Fig. 2.** Two kinds of aluminum rods were used: one is 50 mm in length and 1.6 mm in diameter; the other is 50 mm in length and 3.0 mm in diameter. The rods were mixed to form the model ground in such a way that the weight ratio of the former to the latter was equal to 3 to 2. Bi-axial

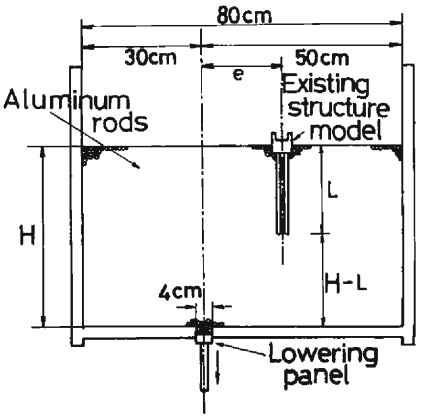

Fig. 2 Sketch of model test apparatus

compression tests were carried out on an assembly of aluminum rods to provide data on strength-deformation characteristics of the model ground. The stress-strain relationships and failure criterion of the assembly of aluminum rods are given in Appendix.

A pile foundation with footing was used as the existing foundation model. The detailed dimension of the pile-foundation model is shown in **Fig. 3.** The penetration depth of this pile foundation, L, was chosen at a fixed value of $L=22$ cm.

Two series of lowering-panel tests were performed. In the first series of lower-

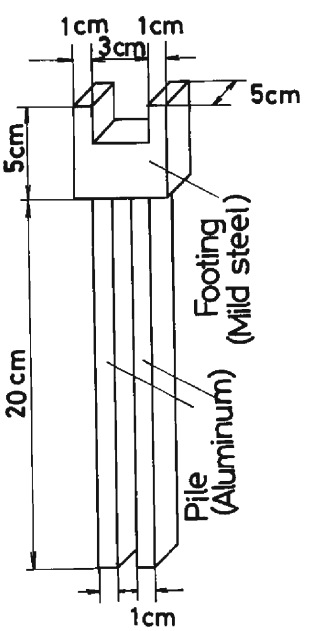

Fig. 3 Detail of the pile foundation

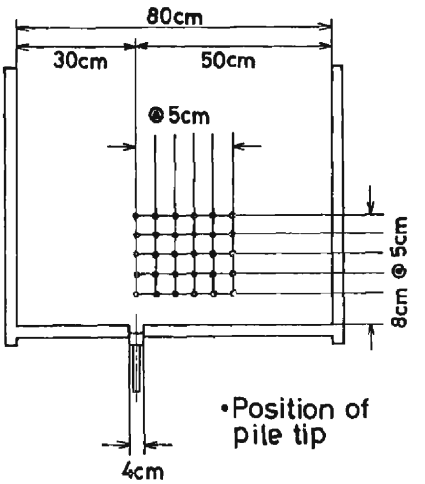

Fig. 4 Position of the end of the pile in series-1 model tests

ing-panel tests, the overburden, H, and the horizontal distance, e, between the center of the lowering-panel and that of the pile foundation were chosen as the testing variables. A total of 30 cases of model tests were carried out; Five cases of overburden were considered, i.e., 30 cm, 35 cm, 40 cm, 45 cm and 50 cm, and under a fixed overburden (H) six cases of horizontal distance (e) were selected, i.e., 0 cm, 5 cm, 10 cm, 15 cm, 20 cm and 25 cm (see **Fig. 4**). In the second series of lowering-panel tests, the model pile was not installed in the assembly of aluminum rods, to provide reference data on soil movements above the lowering-panel.

The vertical displacement at the top of the model pile was measured with two dial-gauges (sensitivity: 1/100 mm) and the horizontal displacement of the model pile was measured with a potentiometer (sensitivity: 1/500 mm). Note here that the model pile moves as a rigid body because of its high flexural rigidity employed. Thus, the vertical displacement on top of the pile, δ_F, is defined as $\delta_F=(\delta_{F1}+\delta_{F2})/2$, and the horizontal displacement of the footing as d_F (see **Fig. 5**). The elevation view

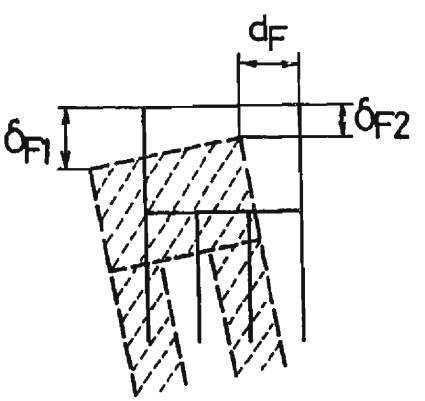

Fig. 5 Displacement of the pile footing

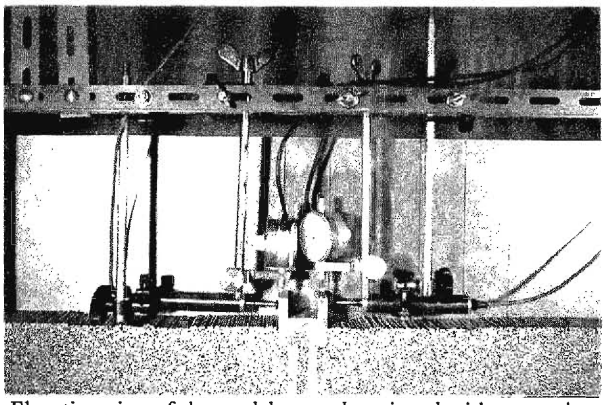

Photo. 1 Elevation view of the model ground equipped with measuring apparatus

of the model ground equipped with these measuring apparatus is shown in **Photo. 1**.

The displacement field of the model ground was measured by means of a photographic technique. That is to say, after taking pictures of the vertical section of an assembly of aluminum rods, those films were enlarged to (25.4×30.5 cm) size and the values of displacements at selected points in the model ground were read on a digitizer.

The photographic and reading conditions adopted are as follows.

Camera	: Nikkon F2 photomic A
Lens	: NIKKOR (35 mm, F1.4)
Film	: FUJI NEOPAN SS ISO 100
Distance between camera and model	: 1 m
Iris	: F4
Shutter speed	: 1/60 sec.
Enlarged ratio	: 10.5 times
Sensitivity of the digitizer	: 0.1 mm

The Test procedure adopted is as follows. Firstly, a rear steel plate is temporarily set between the right and left boundary walls of the container. The pile with a footing is then fixed on this plate at a prescribed position, with the aid of a magnet which is placed behind the rear steel plate. At this stage, the verticality of the pile foundation should be ensured by means of a water level. Next, aluminum rods are piled up with their axes horizontal, to a prescribed height. After the prescribed overburden is reached, the marking lines are drawn on the vertical face of the assembly of the aluminum rods. Then, the dial-gauges and the potentiometer are put into position. Finally, the rear steel plate and the magnet for the cramp are removed. A photograph of the initial state is taken at this stage and then the lowering-panel is allowed to settle at a given rate. Measurements of the vertical and horizontal displacements of the footing are taken at every 1 mm-settlement of the lowering-panel, whereas pictures of the model ground are taken at every 2 mm-settlement of the lowering-panel, until a final, prescriebd settlement of 20 mm is

reached.

2.2 Test Results and Discussion

(1) The Displacements of Pile Foundation Induced by the Settlement of the Lowering-Panel

Let us first consider the development of the settlement of the piled footing, δ_F, with the settlement of the lowering-panel, δ_L.

Fig. 6 shows the effect of overburden, H, on the relation between δ_F and δ_L, when the pile foundation was located right above the lowering-panel, i.e., $e=0$. It is seen that the settlement of the footing, δ_F, increases remarkably with that of the lowering-panel, δ_F, when the overburden, H, is smaller than or equal to 35 cm ($H/B=8.75$). When the overburden, H, is relatively large ($H=40$ cm or $H=45$ cm), δ_F appears to increase proportionally to δ_L, and at the largest overburden depth of $H=50$cm, the pattern appears to be followed by a tendency for δ_F to level off at large values of δ_L.

Fig. 7 shows the effect of the distance (e) between the pile and lowering-panel upon the rate of development of δ_F against δ_L, for a minimum overburden depth

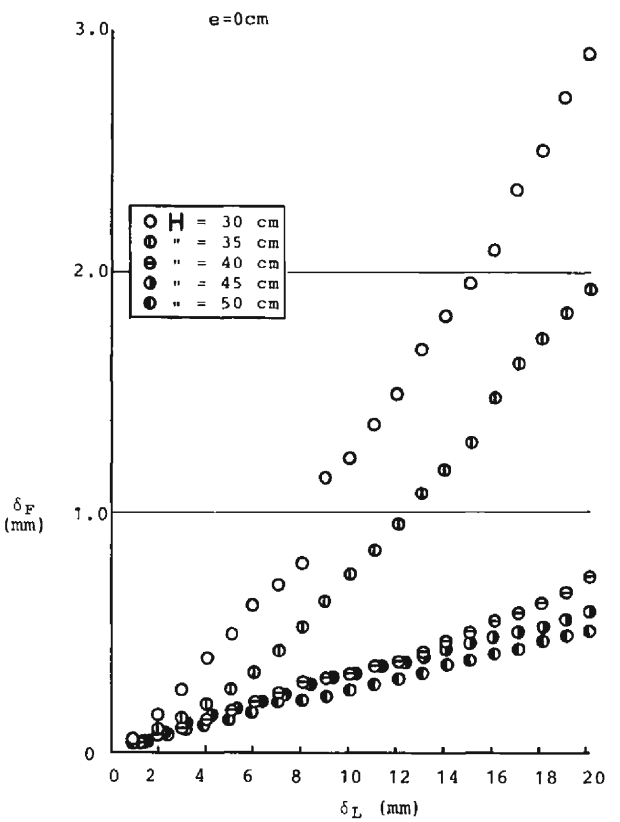

Fig. 6 Relation between δ_F and δ_L for $e=0$ cm

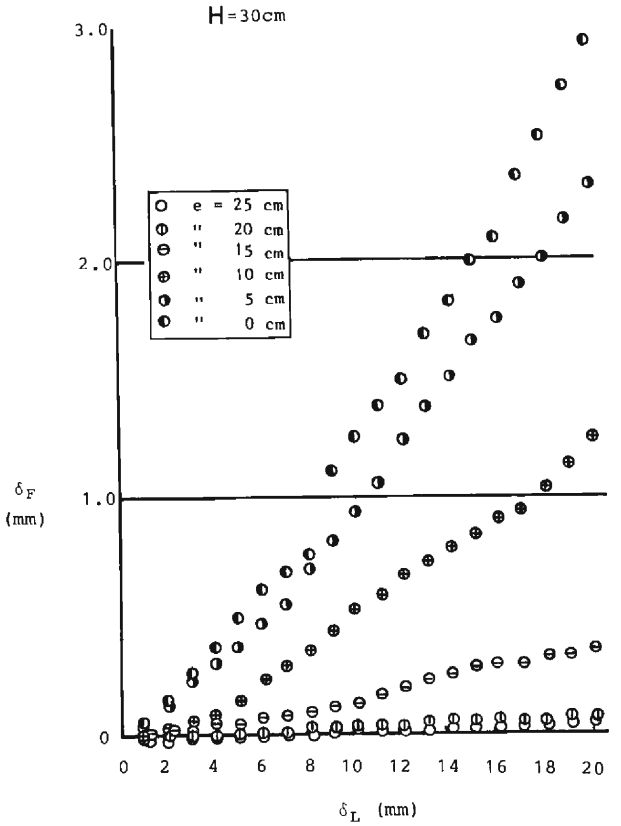

Fig. 7 Relation between δ_F and δ_L for $H=30$ cm

of $H=30$ cm ($H/B=7.5$). It is seen that δ_F increases remarkably with increase of δ_L when $e=0$ or $e=5$ cm. This tendency, however, appears to be suppressed rapidly with increasing horizontal distance (e). In fact, it is interesting to note that when $e \geqq 15$ cm, δ_F tends to level off at large values of δ_L.

In view of the results shown in **Figs. 6** and **7**, it may be possible to classify the pattern of development of δ_F with δ_L into such as shown in **Fig. 8**. Pattern 1 represents the relation which occurs when both the overburden depth (H) and the horizontal distance (e) are small; in this case, the settlement of the ground as well as that of the footing is noted to increase remarkably with the settlement of the lowering-panel. Pattern 3 shows the relation which prevails when either the overburden depth (H) or the horizontal distance (e) is sufficiently large; in this case the settlement of the footing is noted to converge gradually at a certain finite value. Pattern 2 shows the relation which is seen when both the overburden depth (H) and the horizontal distance (e) are intermediate in value; in this case, δ_F increases in proportion to δ_L and in this sense this behavior may be regarded as quasi-elastic.

Next, let us consider the horizontal movement of the pile which is also associated with the settlement of the lowering-panel. **Fig. 9** exemplifies the relations between

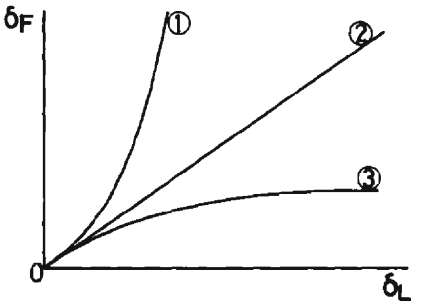

Fig. 8 Classification of the relation between δ_F and δ_L

the lateral displacement of the footing, d_F, and δ_F, for a fixed value of H=35 cm. Let us first look at the case when e=0. In this case, as expected, δ_F is seen to increase with no development of d_F. It is then noted that as e becomes larger, the slope of the line between d_F and δ_F becomes steeper. This means that the role of the lateral displacement becomes more significant, in the case where e is great. This statement is reinforced more clearly from **Fig. 10**, in which four equi-contour lines of d_F/δ_F are drawn as an e versus H diagram.

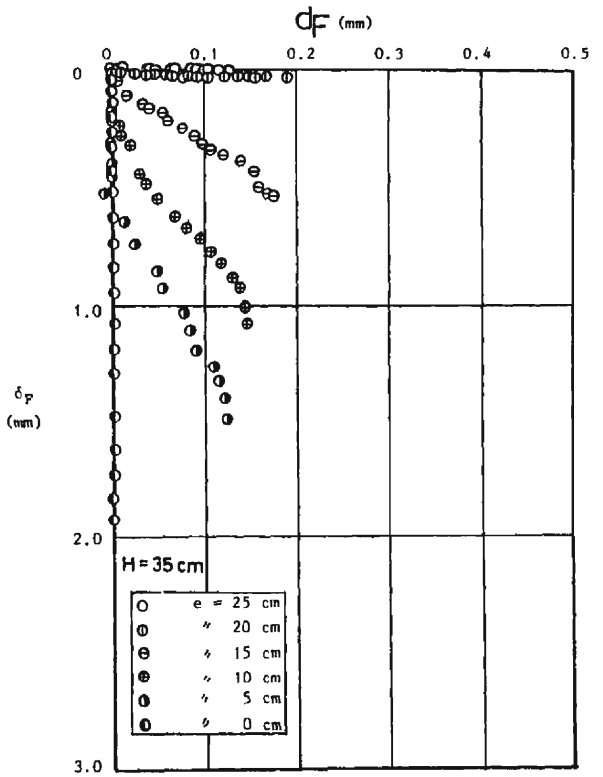

Fig. 9 Relation between d_F and δ_F for H=35 cm

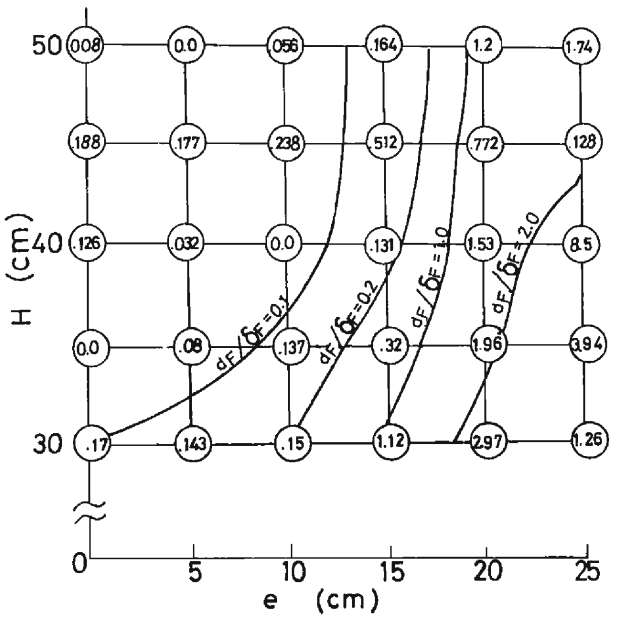

Fig. 10 Equi-contour lines of d_F/δ_F on $e\sim H$ surface

(2) The Displacement Field of the Ground above the Lowering-Panel

In this section we will first consider the development of the ground movements with the settlement of the lowering-panel, on the basis of results from the series-2 experiments. We will then consider the effect of the presence of the pile foundation on the displacement field in the ground, by comparing the experimental results from series 2 with those from series 1.

Figs. 11 show the development of the equi-settlement contour lines with the settlement of the lowering panel, for a given overburden depth of $H=30$ cm. Hereafter, the value of equal-settlement is indicated in millimeters (mm) by the number enclosed with the open circle. From these figures, it is seen that the region of

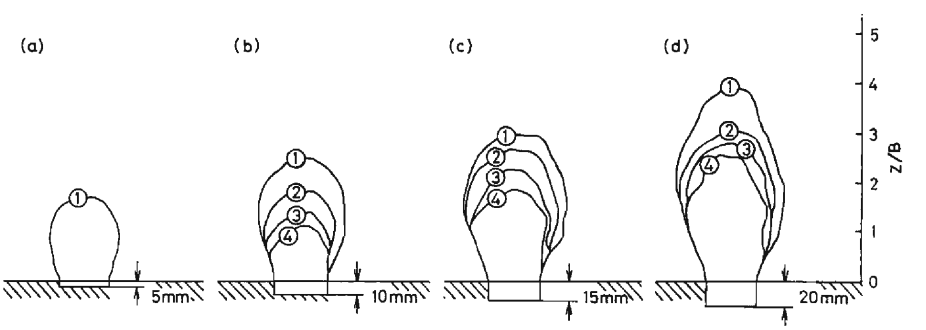

Fig. 11 Development of the equi-settlement contour lines with the drop of the lowering panel for $H=$ 30 cm

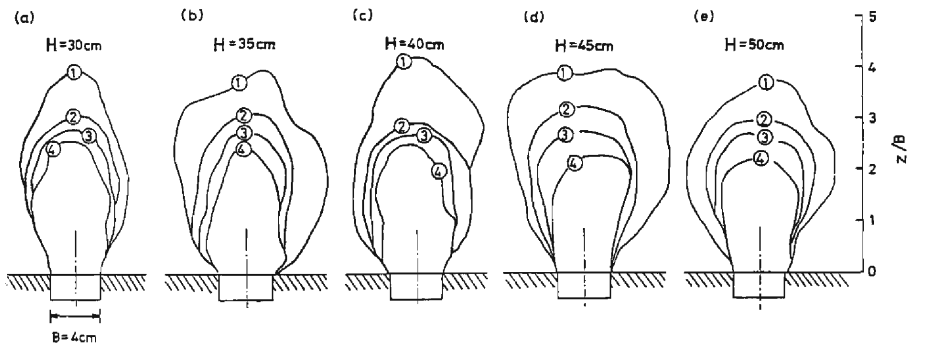

Fig. 12 Equi-settlement contour lines at $\delta_L=20$ mm

influence of the each equi-settlement contour line becomes larger with the settlement of the lowering-panel; this is most clearly seen by taking note of equal 1 mm-settlement.

Figs. 12 show the equi-settlement contour lines at five different values of the overburden depth (H), when the settlement of the lowering-panel, δ_L, reaches 20 mm for every overburden depth. From these figures, it is seen that, as expected, the equi-settlement contour lines are practically symmetric with respect to the central axis of the lowering panel. Also, it is of interest to mention that the equi-settlement contour line of 1 mm reaches a point approximately 4B above the lowering-panel, irrespective of the magnitude of overburden depth (H). This suggests that the present experimental program, in which $H \geqq 7.5$B throughout, is concerned exclusively with the situation of "deep tunnel"[5].

Figs. 13 show the development of the equi-settlement contour lines in the model ground with the lowering-panel settlement (δ_L), under conditions of $H=30$ cm and

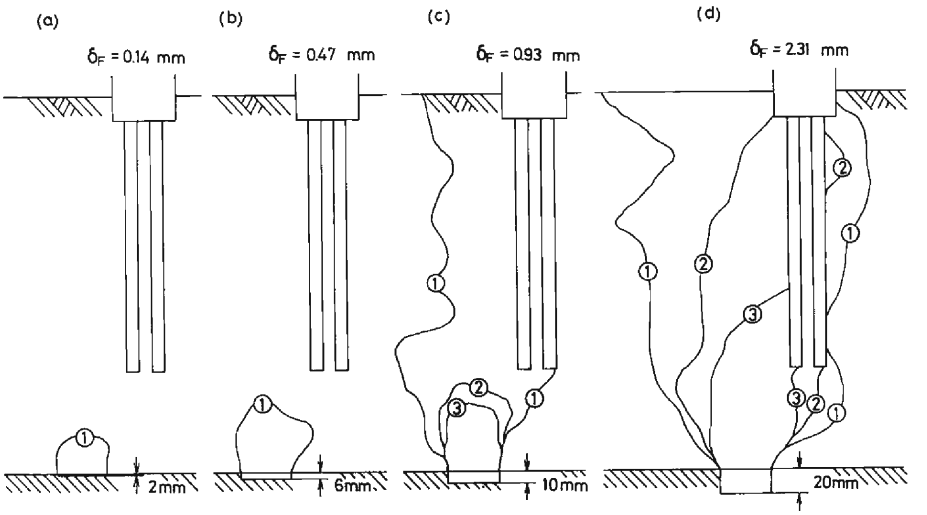

Fig. 13 Development of the equi-settlement contour lines for $H=30$ cm and $e=5$ cm

e=5 cm. It is seen that the presence of the pile foundation does not exert a significant influence on the 1 mm settlement contour as long as the value of δ_L is small. When the settlement of the lowering-panel reaches 10 mm, the equi-settlement contour lines are seen to be disturbed to some extent, and the equi-settlement contour line of 1 mm is noted to come up to the ground surface. The disturbance of this tendency is seen to become more significant for contour lines as the lowering-panel settlement approaches 20 mm.

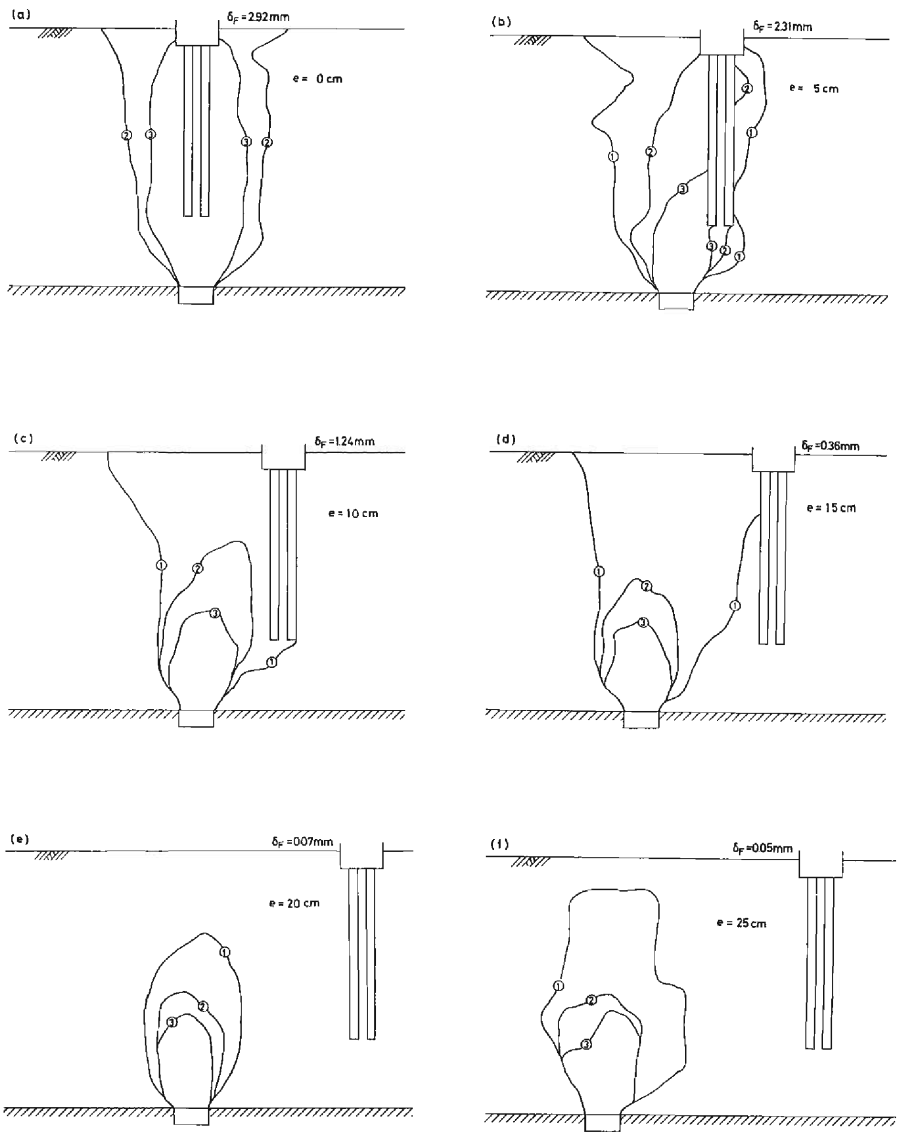

Fig. 14 Equi-settlement contour lines at δ_L=20 mm, for six different offsets (e); (a) e=0 cm, (b) e=5 cm, (c) e=10 cm, (d) e=15 cm, (e) e=20 cm and (f) e=25 cm

Figs. 14 show the equi-settlement lines at six different values of the horizontal distance (e), for a fixed value of H=40 cm, when the settlement of the lowering-panel reaches 20 mm. Let us first consider the results for e=0 (see **Fig. 14(a)**). From this figure, it is seen that the equi-settlement contour lines of 2 mm and 3 mm reach the ground surface, in marked contrast with the results shown in **Fig. 12(c)** for H=40 cm where no pile foundation was installed in the ground. In other words, this finding means that the presence of the pile foundation interrupts the formation of the so-called "ground arch" within which the ground deformations tend to be localized.

Fig. 14(b) shows the equi-settlement contour lines for e=5 cm. It is seen that the presence of the pile foundation leads to the unsymmetric pattern of the deformation field. It is also noted that the equi-settlement contour line of 1 mm comes up to the ground surface. **Figs. 14(c)** and **(d)** show the results for e=10 cm and e=15 cm, respectively. It is noted here that the equi-settlement contour lines of 2 mm and 3 mm are closed. Similar pattern is recognized for e=15 cm, as shown in **Fig. 14(d)**. The results for larger horizontal distances (e=20 cm and e=25 cm) are shown in **Figs. 14(e)** and **(f)**. In these figures, it is seen that the equi-settlement contour lines of 3 mm, 2 mm and 1 mm are all closed. This suggests that the ground arch is formed. It is also important here to note that in those situations where the pile is located far away from the ground-arch formed, the pile settlements are very small; in fact, δ_F=0.07 mm for e=20 cm and δ_F=0.05 mm for e=25 cm.

(3) Transversal Settlement in the Ground

In this sub-section, let us discuss the distribution of settlements within the ground, with reference to Eq. (1). As mentioned earlier, Eq. (1) was originally proposed to estimate the transversal settlement at the ground surface. In this study we attempt to modify this equation to describe the transversal settlement at any point within the ground. That is to say, we use the lowering-panel settlement, δ_L, instead of the parameter, δ_T, and the width of the lowering panel, B, for the tunnel radius, a. Also the vertical distance to a point within the ground from its bottom is denoted by z ($0 \leqq z \leqq H$). Thus, Eq. (1) is transformed into:

$$\delta(x, z)=\delta_0(z/B, \delta_L)\cdot\exp[-c_3\cdot(x/z)^2] \quad \cdots\cdots (2)$$

in which

$$\delta_0(z/B, \delta_L)=C(\delta_L)\cdot\exp[-c_4\cdot(z/B)] \quad \cdots\cdots (3)$$

Here, $\delta_0(z/B, \delta_L)$ is the settlement along the central axis of the lowering-panel and is thought as functions of z/B and δ_L. The coefficient $C(\delta_L)$ in Eq. (3) is a proportional coefficient depending on the magnitude of δ_L. Both c_3 and c_4 are constants to be determined experimentally.

Let us first check the validity of Eqs. (2) and (3) against the experimental results for the case where the pile foundation was not installed.

Fig. 15 shows the experimental results plotted in the form of log (δ_0/δ_L) against z/B. From this figure, it is recognized that there is a good linear relation

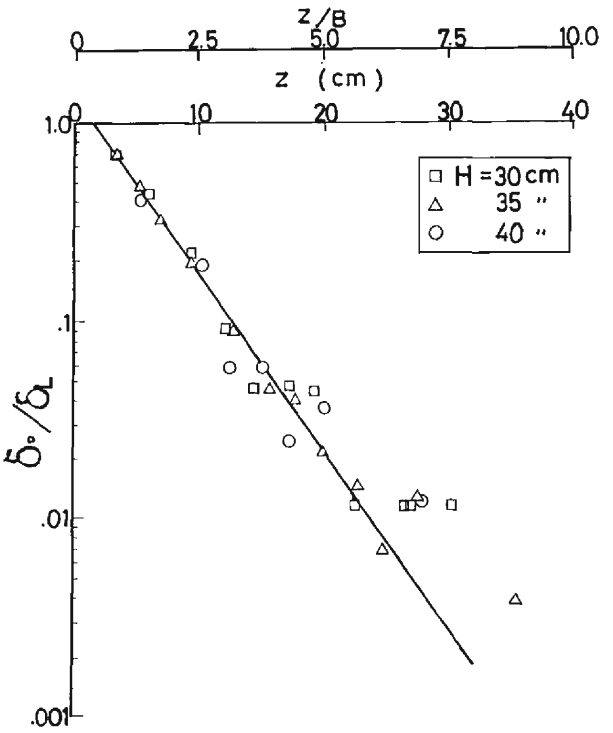

Fig. 15 Relation between log $((\delta_0/\delta_L))$ and z/B

between $\log(\delta_0/\delta_L)$ and z/B, as expected from Eq. (3). The experimental results for $\delta_L=20$ mm were plotted in **Fig. 16**, in the form of $\log(\delta/\delta_0)$ against

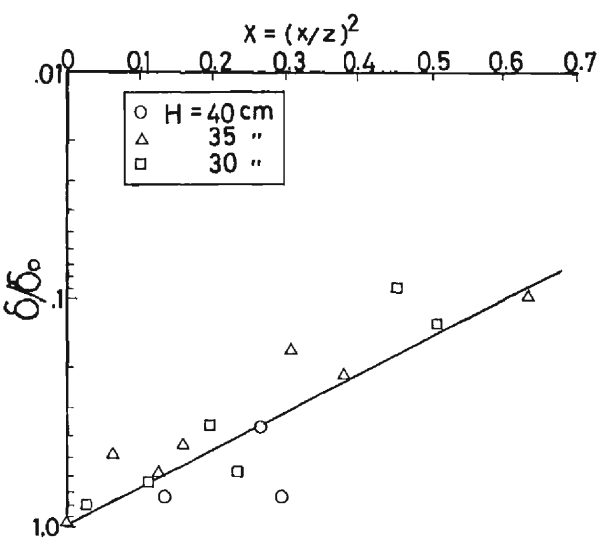

Fig. 16 Relation between log (δ/δ_0) and $(x/z)^2$

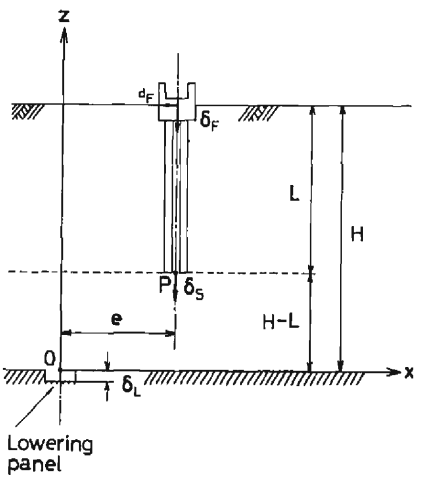

Fig. 17 Main parameters used in this section

$(x/z)^2$. From this figure, it is evident that $\log(\delta/\delta_0)$ is proportional to $(x/z)^2$, as expected from Eq. (2). In view of these results, it may be concluded that Eqs. (2) and (3) are valid to estimate the settlement at any position in the model ground above the lowering panel.

Let us now introduce a parameter denoted by δ_s, which represents the settlement at point P just below the pile tip (**Fig. 17**). In view of the results described above, the value of δ_s may be estimated by substituting $x=e$ and $z=H-L$ into Eqs.

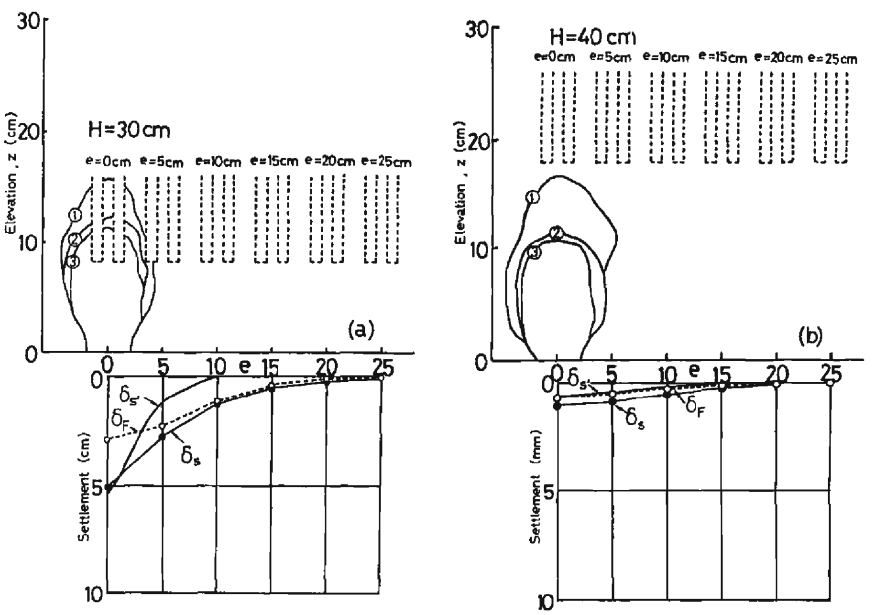

Fig. 18 Plots of δ_s, δ_s', and δ_F in relation to e

(2) and (3). Hereafter, let us denote this estimated settlement as δ_s'. In what follows, we will discuss the relation among the ground settlement (δ_s) measured at point P, the ground settlement $(\delta_s)'$ estimated by Eqs. (2) and (3), and the footing settlement (δ_F) measured at the top of the piled footing.

Fig. 18(a) gives plots of δ_s, $\delta_{s'}$ and δ_F against the horizontal distance (e), for $H=30$ cm. In this figure, the equi-settlement contour lines obtained for the case where the pile foundation was not installed in the model ground, are also plotted for the purpose of explanation. From this figure it is seen that δ_s' decays to zero, at $e \geqq 10$ cm, whereas δ_s decreases more slowly owing to the presence of the pile foundation. More specifically, in this overburden depth of $H=30$ cm, the presence of the pile foundation is thought to have disturbed the formation of "ground arch" and have consequently resulted in greater settlements, as exemplified by the relation $\delta_s > \delta_{s'}$. The reason for $\delta_F > \delta_{s'}$ at $e \leqq 5$ cm is difficult to determine at the present stage. However, the results shown in **Figs. 14(a)** and **(b)** suggest that the pile is supported by the upper portion of its surrounding ground.

Fig. 18(b) shows the results for $H=40$ cm. From this figure it is seen that the value of δ_F almost coincides with the value of $\delta_{s'}$ for each horizontal distance (e). In this overburden depth of $H=40$ cm, the pile base is considered to be sufficiently remote from the lowering-panel, such that the "ground arch" is formed. Therefore, in a practical sense, we can make the following approximation: $\delta_F \simeq \delta_s \simeq \delta_{s'}$. This means that there is a possibility to estimate the settlement of the existing pile foundation on the basis of Eqs. (2) and (3).

When we apply these equations to prototype problems, however, we must keep in mind the difference in size between the model and prototype structures. Furthermore, the behavior of the sandy ground, where the discontinuous nature of deformations such as the formation of "ground arch" is representative, has been hitherto known to be very difficult to reproduce by means of a continuum-mechanics approach. Therefore, in the next section, we will show how a new finite element model can describe the displacement field of the granular medium above a lowering-panel or yielding base.

3. Analytical Studies

3.1 Analytical Methods

In view of the results obtained from the model tests, we must choose the numerical method which can describe the discontinuous nature of the deformation field. To fulfill this requirement, we decided to use a newly developed analytical procedure[5], in which all the ordinary triangular finite elements are covered with joint elements[6] (see **Fig. 19**).

In what follows, we will first compare the results from such joint element analyses (J.E.A.) with those from the usual non-elastic element analyses (N-E.E.A.). Next, we will compare the results from J.E.A. with the experimental results described in the previous sections, and will discuss how J.E.A. can reproduce the experimental results.

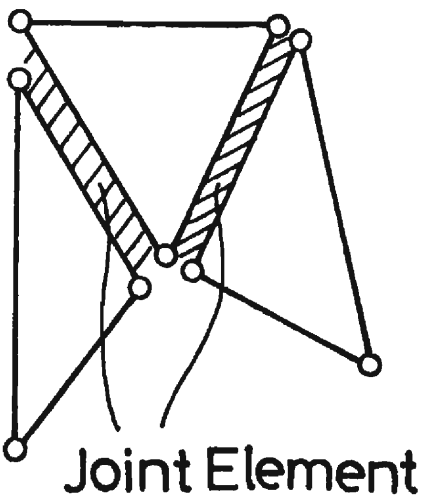

Fig. 19 Joint elements placed on all of the boundaries of triangular elements

A finite element mesh used is shown in **Fig. 20**. This is essentially the same for J.E.A. and N-E.E.A. The initial stress state in the model ground was assumed to be K_o-condition ($K_o=0.5$). The material parameters for an assembly of aluminum rods used in the analyses were obtained from the bi-axial compression tests (see Appendix) and summarized in **Table 1.** In the process of numerical calculation, the prescribed displacements were given for the nodal points on the lowering-panel in 20 steps until the settlement of the lowering-panel reached 20 mm.

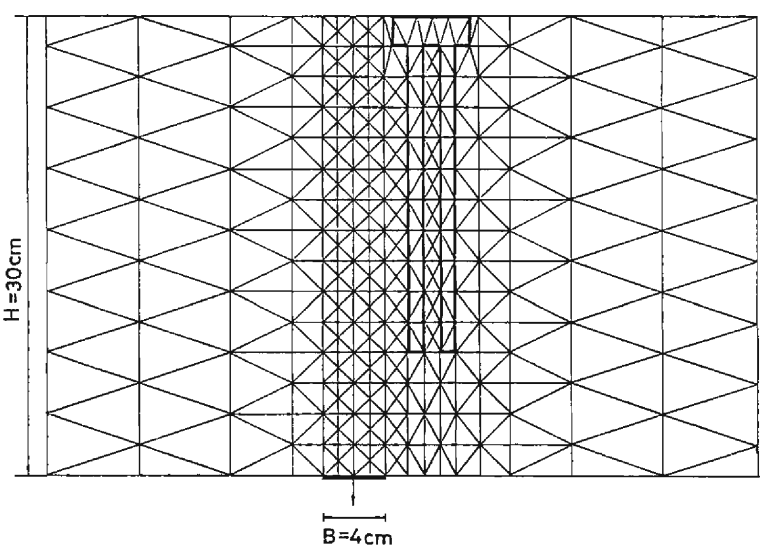

Fig. 20 Finite element mesh used in this study

Table 1 Material parameters used in the analyses

	Aluminum
Unit Weight γ (gf/cm^3)	2.18
Young's Modulus E (gf/cm^2)	$500+10^2\sigma_m$
Poisson's Ratio ν	1/3
Cohesive Strength c (gf/cm^2)	0
Internal Friction Angle ϕ (°)	30
Coefficient of Earth Pressure at Rest K_0	0.5

3.2 Analytical Results and Discussion

Fig. 21 shows the caluculated results from J.E.A. for the case where the pile foundation was not installed in the model ground, for an overburden depth of $H=$ 30 cm, whereas **Fig. 22** shows those from N-E.E.A. under the same condition. It is seen that the region of the influence of each equi-settlement contour spreads with increasing settlement of the lowering-panel. In J.E.A., the formation of "ground arch" is well reproduced and the influence region tends to remain localized. In contrast, the influence of equi-settlement contour predicted from N-E.E.A. tends to extend considerably a long distance, without a sign of the formation of "ground arch".

Figs. 23 and **24** show the analytical results for the case where the pile foundation was instaled in the model ground, under conditions of $H=30$ cm and $e=5$ cm. From **Fig. 23**, it is seen that the contour of equal 0.5 mm-settlement reaches the ground surface at $\delta_L=20$ mm, whereas in **Fig. 24**, the contour of equal 0.5 mm-settlement forms a loop near the pile tip.

The differences in predicted patterns of distribution of ground movements are more clearly seen from **Figs. 25** and **26**, where the transversal settlements calculated from the two methods are shown. It is seen from **Fig. 25** that the localization of the ground settlements just above the lowering-panel is well reproduced in J.E.A. as compared with N-E.E.A. Also, it is seen that at upper levels of the ground, the

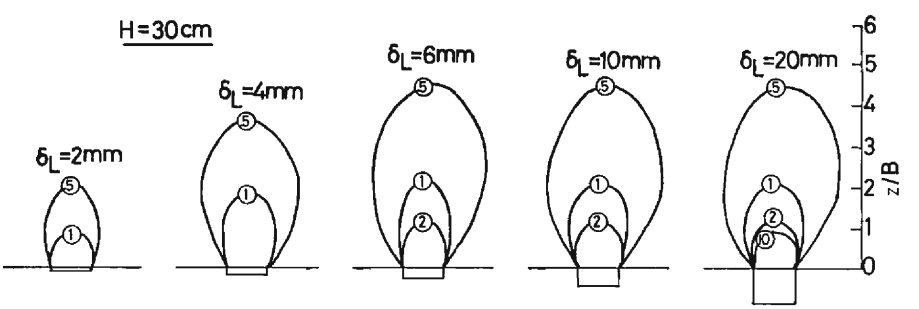

Fig. 21 Development of the equi-settlement contour lines from J.E.A. for the case where the pile foundation was not installed

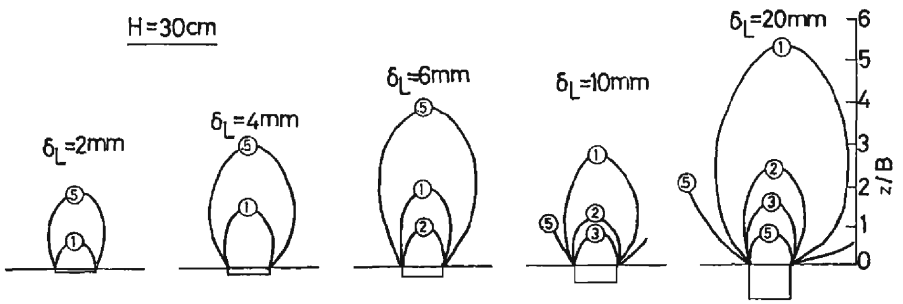

Fig. 22 Development of the equi-settlement contour lines from N-E.E.A. for the case where the pile foundation was not installed

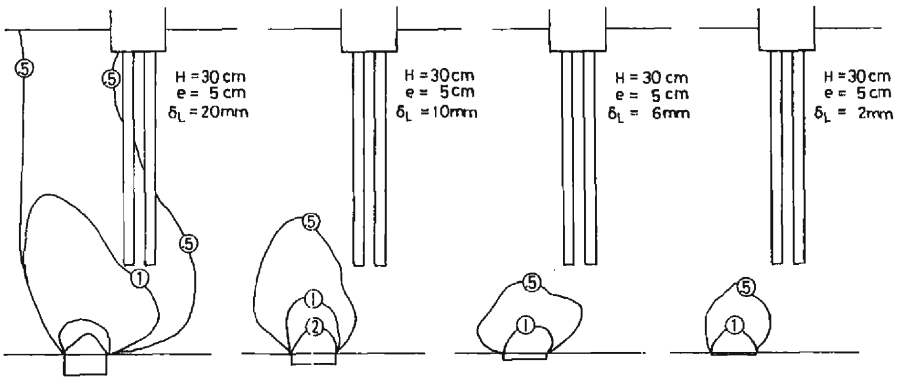

Fig. 23 Development of the equi-settlement contour lines from J.E.A. for the case where the pile foundation was installed

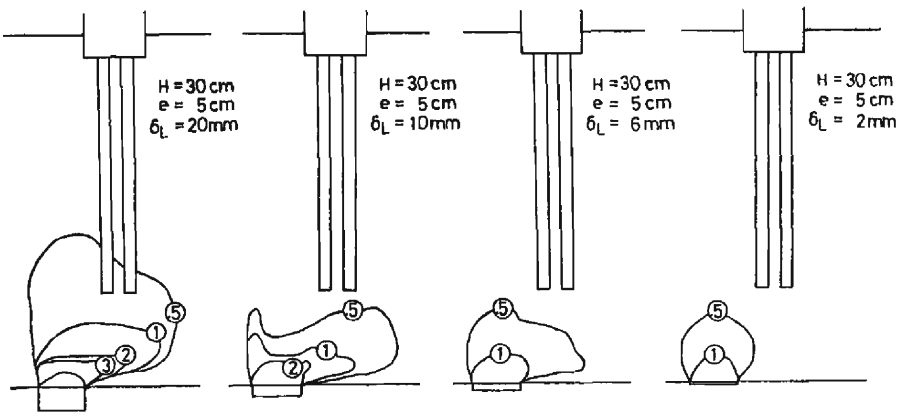

Fig. 24 Development of the equi-settlement contour lines from N-E.E.A. for the case where the pile foundation was installed

settlements decay more rapidly in J.E.A. than in N-E.E.A. This fact means that the localization of the ground movement within "ground arch", which has been observed in the model tests, is well reproduced in J.E.A.

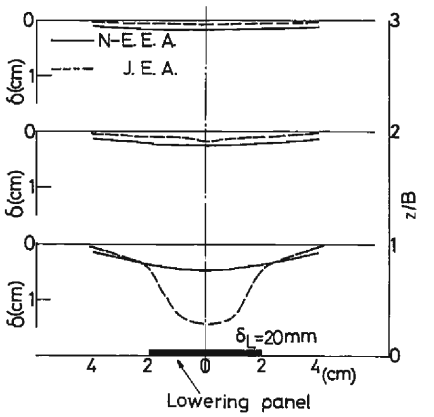

Fig. 25 Transversal settlements calculated for the case where the pile foundation was not installed

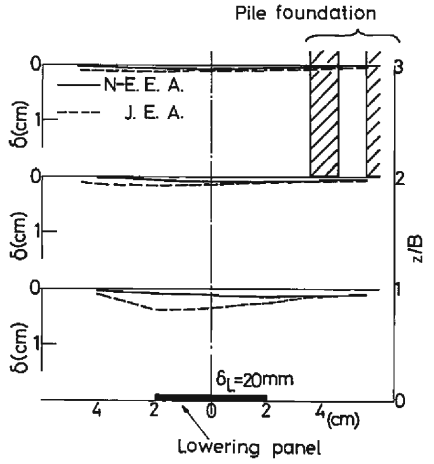

Fig. 26 Transversal settlements calculated for the case where the pile foundation was installed

The transversal settlements predicted for the case where the pile foundation is installed in the model ground, are seen to be unsymmetric due to the presence of the pile foundation (**Fig. 26**). Note that this predicted pattern of deformation is compatible with what has been observed in the model tests, and that the effect of the presence of the pile foundation on the settlement pattern is more realistically reproduced in J.E.A. than in N-E.E.A.

4. Conclusions

The main results obtained from the present study are summarized as follows.

(1) The relations between the settlement of the footing, δ_F, and the lowering-panel settlement, δ_L, have been classified into three patterns as shown in **Fig. 8**. Pattern 1 is characterized by the property that δ_F accelerates with increasing δ_L

under the condition that both H and e are small. Pattern 2 is characterized by the property that δ_F increases in proportion to δ_L under the condition that both H and e are medium. Pattern 3 is characterized by the property that δ_F levels off gradually with increasing δ_L. This occurs under the condition that either H or e is large.

(2) As the horizontal distance, e, becomes larger, the lateral displacement of the pile foundation becomes more remarkable than the vertical movement.

(3) If there is no existing pile foundation and the overburden, H, is sufficiently large, the ground arch is formed above the lowering-panel, and only the minor deformations develop in the region beyond it.

(4) If the pile foundation exists near the lowering-panel, the formation of ground arch is disturbed and a large deformation takes place.

(5) Distributions of settlement within the ground above the lowering-panel are expressed in the form of Eqs. (2) and (3); The validity of these equations are confirmed on the basis of the results from series-2 experiments.

(6) The joint element analysis (J.E.A.) is ascertained to reproduce realistically the displacement field within the granular medium undergoing the lowering-panel settlement, together with a qualitatively good description of the disturbance effect of the pile presence with respect to the formation of ground arch.

Acknowledgements

The authors wish to express their heartfelt thanks to Prof. H. Matsuoka, Nagoya Institute of Technology, for his helpful support and advice in conducting the bi-axial compression tests on the assembly of aluminum rods. Thanks are also extended to Mr. M. Mimura and Mr. M. Nagataki for their helpful support in conducting the model tests and improving the measuring techniques.

All the computations reported in this paper were performed at the Data Processing Center, Kyoto University.

References

1) Peck, R.B.: Deep Excavations and Tunnelling in Soft Ground, Proc. 7th ICSMFE, Mexico City, Mexico, 1969, pp. 225–290.
2) Attewell, P.B. and Taylor, R.K. (Ed.): Ground Movements and their Effects on Structures, Surrey University Press, USA, Chapman & Hall, New York, 1984.
3) Shimada, T.: Surface Settlement above the Conventionally Excavated Tunnels with Thin Earth Cover, Proc. JSCE, No. 296, 1980, pp. 97–109 (in Japanese).
4) Murayama, S. and Matsuoka, H.: On the Settlement of Granular Media Caused by the Local Yielding in the Media, Proc. JSCE, No. 172, 1969, pp. 149–159 (in Japanese).
5) Adachi, T., Tamura, T., Yashima, A. and Ueno, H.: Behavior and Simulation of Sandy Ground Tunnel, Proc. JSCE, No. 358, 1985, pp. 129–136 (in Japanese).
6) Goodman, R.E. and St. John, C.: Finite Element Analysis for Discontinuous Rocks. In: Numerical Methods in Geotechnical Engineering, McGraw-Hill, 1977, pp. 157–165.

Appendix—Strength-Deformation Characteristics of Model Ground

Bi-axial compression tests of an assembly of aluminum rods were carried out to understand strength-deformation characteristics of model ground. Here, we show the experimental results. **Fig. A–1** shows stress-strain relations and **Fig. A–2** shows the failure criterion.

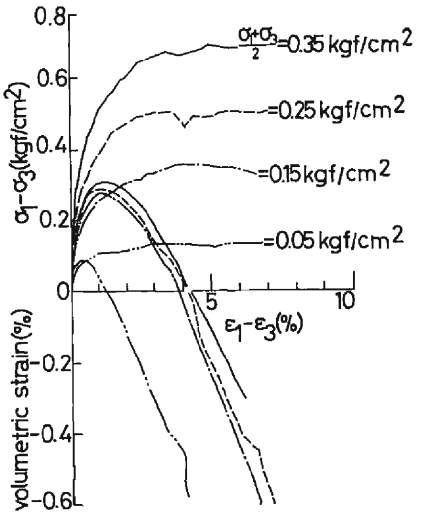

Fig. A–1 Stress-strain relations of an assembly of aluminum rods

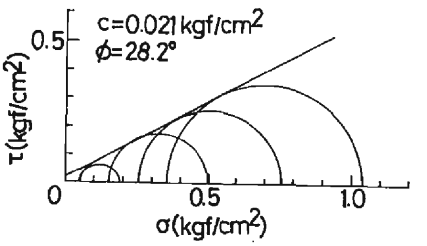

Fig. A–2 Failure criterion of an assembly of aluminum rods